A revised solid-state NMR method to assess the crystallinity of cellulose

(article starts on next page)

A revised solid-state NMR method to assess the crystallinity of cellulose

Tobias Sparrman · Leo Svenningsson · Karin Sahlin-Sjövold · Lars Nordstierna ·
Gunnar Westman · Diana Bernin[iD]

Abstract The crystallinity of cellulose has a strong impact on various material properties. Over the years, many methods have become available to estimate the crystallinity. The purpose of this work was to revise existing NMR-based methods and to introduce a complementary NMR method related to the ^{13}C T_1 relaxation time. The ^{13}C T_1 differs by an order of magnitude for amorphous and crystalline polymers among them cellulose. We have utilized the signal boost of ^{1}H–^{13}C cross polarization and the difference in ^{13}C T_1 as a filter to calculate the degree of crystallinity. The evaluation of the method is based on the difference in peak integrals, which is fed into a simple equation. The method was applied to five cellulosic samples of different nature and compared the obtained degree of crystallinity with the degree estimated from deconvoluted X-ray scattering patterns. Furthermore, an attempt has been made to give a basic understanding on the origin of CP enhancement in order to validate various proposed NMR methods. With the recent progress of NMR equipment, the presented method can be automatized and applied to a series of samples using a sample changer.

T. Sparrman (✉)
Department of Chemistry, Umeå University, Umeå,
Sweden
e-mail: tobias.sparrman@umu.se

L. Svenningsson · K. Sahlin-Sjövold ·
L. Nordstierna · G. Westman · D. Bernin (✉)
Department of Chemistry and Chemical Engineering,
Chalmers University of Technology, Göteborg, Sweden
e-mail: diana.bernin@chalmers.se

K. Sahlin-Sjövold · L. Nordstierna · G. Westman
Wallenberg Wood Science Center, Chalmers University
of Technology, Göteborg, Sweden

D. Bernin
Swedish NMR Centre, University of Gothenburg,
Göteborg, Sweden

Introduction

Cellulose comprises a major fraction in cell walls in wood and is the most abundant biopolymer. This linear polymer based on polysaccharides has excellent material properties when aggregated into hierarchical structures. The polysaccharide chains pack in crystalline and/or amorphous structures and the ratio of these depends on its origin and/or treatment. The native crystalline form is denoted 'cellulose I', which is a combination of two crystalline phases, I_α and I_β, while regenerated celluloses typically contain another

crystalline form denoted 'cellulose II'. The packing of chains and the degree of crystallinity clearly influences material properties and reactivity, which are crucial properties for the development of new functional bio-based materials.

Mechanical and morphological properties correlate well with the degree of crystallinity (Kim et al. 2013; Sixta et al. 2015). Crystalline packing of cellulose chains appears to have an impact on the permeability of gases and water steam in cellulose films (Dufrense 2017) while the size of crystalline domains hampers chemical and biological reactions such as chemical hydrolysis into nanocrystalline cellulose (Klemm et al. 2011) and enzymatic degradation (Klemm et al. 2005; Park et al. 2010; Dufrense 2017). Hence it is important to estimate the degree of crystallinity for raw and modified celluloses and cellulosic materials accurately.

A few common techniques used to determine a degree of crystallinity are Wide Angle X-ray Scattering (WAXS), solid-state NMR spectroscopy and Raman spectroscopy (Evans et al. 1995; Liitiä et al. 2000, 2003; Schenzel et al. 2005; Röder et al. 2006; Park et al. 2009; Park et al. 2010; Ahvenainen et al. 2016). Depending on the method, different procedures analyzing the data have been developed. Some are straightforward and others require advanced analysis and detailed knowledge to apply them successfully. Park et al. (2010) contrasted X-ray and NMR methods on accuracy and utilization (Ahvenainen et al. 2016). Typically, peak intensity and integration routines are preferred due to their inherent simplicity while more demanding evaluation routines based on deconvolution might report values of higher accuracy. The deconvolution routine, described by Larsson et al. (1999) for cellulose I and Idström et al. (2016) for cellulose II, requires excellent signal-to-noise conditions and a ^{13}C spectrum of soaked cellulose, which provides sharper peaks compared to dry cellulose. Both requirements together enable to build meaningful models to estimate the degree of crystallinity, which might however not be applicable to a throughput of a large number of samples.

In solid-state NMR, the experimentally important ^{13}C T_1 parameter has earlier been shown to be sensitive to amorphous and crystalline parts in polymers (Schantz 1997) and cellulosic materials (Teeäär and Lippmaa 1984, Newman and Hemmingson 1994) but requires time-consuming experiments to be used

for routine work. Here, a simple and fast solid-state NMR method based on ^{13}C T_1-filter is presented. Five cellulose samples with different pre-treatment, modification, and dry content were investigated and experimentally compared to other common NMR methods and WAXS.

Materials and methods

Materials

The following five different cellulose rich samples were prepared as follows.

Microcrystalline cellulose (MCC)

Avicell PH-101, with a particle size of approximate 50 μm from Sigma-Aldrich, was used as received.

Soaked MCC (MCC_wet)

MCC_wet was prepared by adding 15 ml deionized water to 2 g of dry MCC. After 24 h, the excess water was decanted and the residual wet MCC was gently squeezed.

Amorphous cellulose (Cell_Am)

Cell_Am was prepared by dissolving and regenerating MCC. 2 g of MCC was added slowly to 15 ml 1-ethyl-3-methylimidazolium acetate (EMIMAc) and stirred at 50 °C overnight. The dissolved cellulose/EMIMAc mixture was poured into ethanol (50 ml) and stirred for 45 min to obtain highly amorphous cellulose (Östlund et al. 2013). The cellulose was filtered and washed with deionized water.

Sulphated nanocrystalline cellulose (CNC-SO_3H)

Sulphated CNC-SO_3H was prepared according to a procedure described by Hasani et al. (2008). In short, MCC was hydrolysed using 64% (wt/wt) sulfuric acid with continuous stirring at 45 °C for 2 h. The reaction was quenched by dilution with deionized water and was dialysed against deionized water, until the conductivity in the effluent remained below 5 μS. The CNC-SO_3H particles were dispersed by sonication at 40% output until a colloidal suspension was achieved

and then freeze dried. For further details, see the supplementary information.

^2H exchanged MCC (MCC$_{ex}$)

1 g of dry MCC was soaked in 10 ml of D_2O. The flask was sealed and let to stand at room temperature to the next day. The water was decanted off and an additional 10 ml of D_2O was added, the flask was sealed and let at room temperature to the next day. The water was decanted off once again and an additional 10 ml of D_2O was added, the flask was sealed and let at room temperature for 4 days. The cellulose was filtered.

The water content was calculated from the difference in weight before and after being dried in the oven at 105 °C for 20 h. MCC had a water content of 4 wt%, MCC$_{wet}$ of 49 wt %, Cell$_{Am}$ of 87 wt%, CNC-SO$_3$H of 14 wt% and MCC$_{ex}$ 4 wt%.

Methods

Wide angle X-ray scattering (WAXS)

Wide angle X-ray scattering measurements was performed with a 0.9 mm beam diameter Rigaku 003+ high brilliance microfocus Cu-radiation source at 132 mm distance from the sample. The experimental duration was approximately 30 min. Many methods exist to quantify the degree of crystallinity, $f_{c.x}$, from WAXS patterns. A regression model of 4 sharp Gaussian (crystalline) signals and one broad Gaussian (amorphous) signal with a linear baseline was applied on the WAXS patterns and an example is shown in Fig. 5. A detailed description and a review of different models and methods to estimate the degree of crystallinity on cellulose using X-ray is reported by Ahvenainen et al. (2016) and Park et al. (2010).

Nuclear magnetic resonance (NMR) spectroscopy

Solid-state NMR experiments were carried out on a Bruker Avance III 500 MHz spectrometer equipped with a 4 mm HX CP MAS probe. Experiments were recorded at a magic angle spinning (MAS) rate of 10 kHz and the temperature was set to 298 K. ^1H decoupling with a "spinal64" (Fung et al. 2000) decoupling scheme at 83 kHz was applied during the acquisition. The duration of the 90° radiofrequency (rf) pulses was 3 µs for ^1H and 4.2 µs for ^{13}C. For the

cross-polarization (CP) experiments, the contact time τ_{cp} was set to 1.5 ms with a ^{13}C rf strength of 60 kHz while ^1H was ramped from 45 up to 90 kHz. This ramp is designed to match both the ± 1 and the ± 2 sideband for the CP transfers at 10 kHz spinning. In combination with the contact time of 1.5 ms, the CP is very stable for small variations for example in tuning. The repetition delay was set to 2 s for all CP experiments. Saturation-recovery experiments (see Fig. 1) were recorded with a repetition time of 2 s and saturation duration of 0.5 ms using an array of 60 consecutive 90° rf pulses with a 4.2 µs delay between them. Direct polarization (DP) experiments were carried out with a 90° rf pulse and a repetition time of 400 s. ^{13}C longitudinal relaxation time (T_1) experiments based on inversion-recovery CP and a saturation-recovery scheme (see Fig. 1) were carried out with 16 delays, t, ranging from 0.1 to 400 s in a logarithmic scale.

The signal intensity I of the T_1 experiments versus the delay t showed a double exponential behavior and was regressed using the following equation
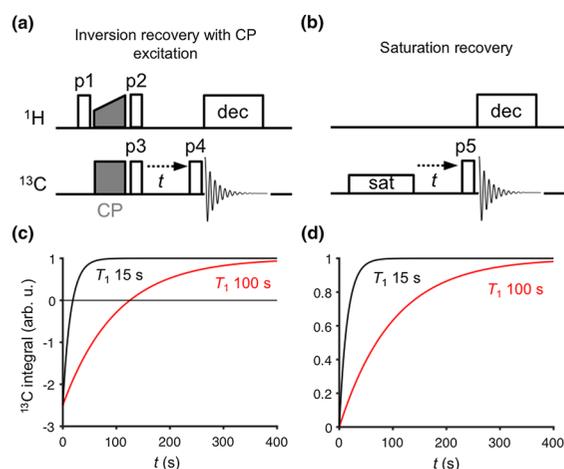

Fig. 1 Top: Pulse sequence schemes to estimate ^{13}C T_1 relaxation times based on an inversion-recovery with CP excitation (**a**) and saturation-recovery (**b**). The rf pulse p1 is a 90° ^1H excitation pulse while p2 is a 90° ^1H flip-back. For ^{13}C, p3 is a 90° rf pulse that inverts the ^{13}C magnetization after the CP transfer while p4 and p5 are 90°s to record the signal, which is ^1H decoupled during acquisition. The saturation block is prior to the delay t. Bottom: Simulated ^{13}C integrals as a function of t for two different T_1s (black: 15 s, red: 100 s) for the inversion-recovery with CP excitation and a CP enhancement e_{CP} of 2.5 (**c**) and saturation-recovery (**d**) experiments
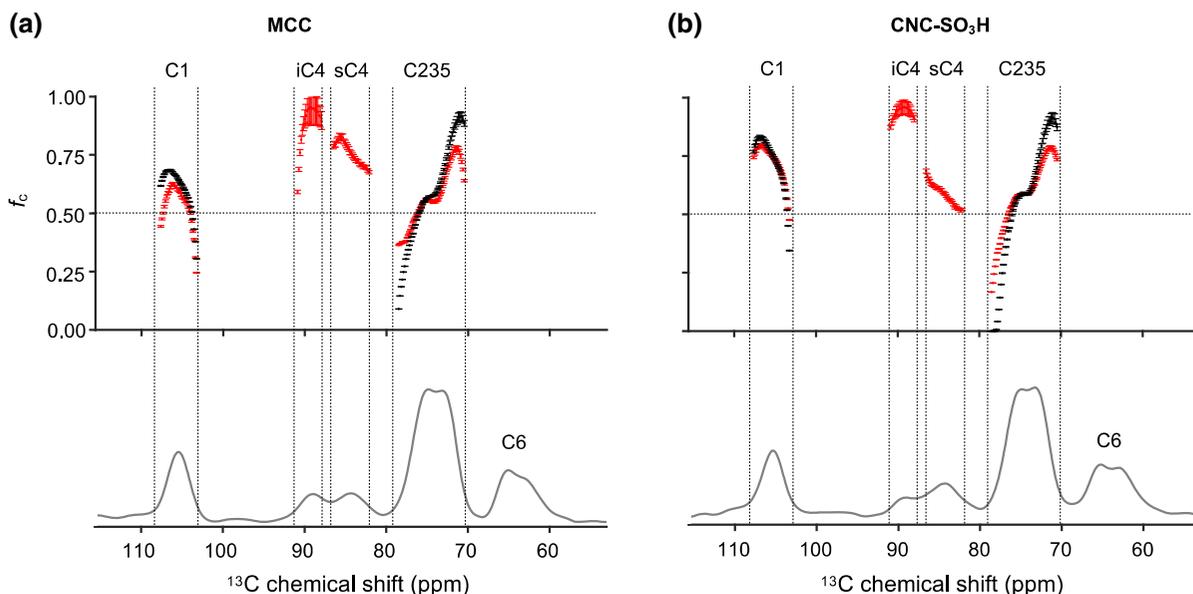
Fig. 2 The degree of crystallinity, f_c, and the CP enhancement, e_{CP}, for each peak region from saturation-recovery (top, red) and inversion-recovery CP T_1 experiments (top, black) for MCC (**a**) and CNC-SO$_3$H (**b**). The error was estimated from 100 Monte–Carlo steps. The f_c-value of C4 for the inversion-recovery CP T_1 experiment could not be estimated due to the weak signal. Assignments of the inversion-recovery CP spectra for the longest delay t were adopted from (Dick-Perez et al. 2011)

$$I = I_0 \left[f_c \left(1 - p e^{-t/T_{1c}} \right) + (1 - f_c) \left(1 - p e^{-t/T_{1a}} \right) \right]$$

(1)

to obtain T_1 for the fractions of 'rigid crystalline', T_{1c}, and 'mobile amorphous', T_{1a}, carbon atoms in the samples. f_c is the fraction of T_{1c} and p is the pre-exponential factor, which is positive for saturation-recovery experiments. For the inversion-recovery CP experiments, p is also positive, and its magnitude is $1 + e_{CP}$, where e_{CP} is the signal enhancement due to CP in comparison to DP. I_0 is the intensity at the time t at which the signal is completely relaxed.

An NMR spectrum is composed of a number of points, which is set prior to the Fourier transform. For pseudo 2D data sets i.e. NMR spectra as a function of a delay, one might integrate the peaks of interest or use each Fourier-transformed point in the peak region to extract the integral/intensity values, which are used for fitting (see Figure S1, Supplementary information). For the saturation-recovery signal intensities, a global fit was performed for each Fourier-transformed point of a peak regions indicated in Fig. 2 using T_{1c} and T_{1a} as global parameters, i.e. one T_{1c} and one T_{1a} value was obtained for each peak region to minimize the number of fitted parameters. The peak regions are highlighted in Fig. 2. f_c and p were allowed to vary, i.e. a f_c and p value was estimated for each Fourier-transformed point. The obtained T_{1c} and T_{1a} relaxation times were used as fixed parameters to fit the inversion-recovery CP signal intensities versus t while f_c and p was allowed to vary for each Fourier-transformed point. The error for the biexponential fitting routine was estimated from 100 Monte–Carlo steps.

For all samples, the degree of crystallinity, $f_{c.int}$, was estimated according to the traditional C4 integration method (Newman 1999) by dividing the integral of the C4 peak resonating at 86.5 to 93 ppm by the integral of the C4 region resonating at 79 to 93 ppm in the corresponding ^{13}C CP NMR spectra. For the MCC$_{wet}$ sample, the degree of crystallinity, $f_{c.dec}$, was estimated by deconvoluting the peaks of the C4 region according to (Larsson et al. 1999; Idström et al. 2016). Here, two new ways are presented of estimating the degrees of crystallinity, $f_{c.inv}$ and $f_{c.sat}$, from the inversion-recovery CP and saturation-recovery experiments. The procedure is explained below.

Theoretical considerations

Dipolar ^1H–^{13}C spin interactions and ^{13}C chemical shift anisotropy (CSA) are the main sources contributing to the ^{13}C T_1 relaxation (Ferreira et al. 2015). For cellulose if not ^{13}C labelled under fast (> 7 kHz) magic angle spinning conditions, the magnitude of the ^{13}C T_1 relaxation time depends mainly on the dipolar interactions, which are dependent on the distance between the ^1H and the ^{13}C nucleus and the rotational correlation time τ_c of the ^{13}C–^1H bond (Nowacka et al. 2013).

Common methods to estimate the ^{13}C T_1 relaxation times are based on an inversion-recovery or a saturation-recovery scheme (see Fig. 1). The inversion-recovery pulse sequence inverts the ^{13}C magnetization, which is routinely excited using a 180° direct excitation rf pulse followed by a delay, t, during which the magnetization is allowed to relax. Depending on the magnitude of the delay and on the ^{13}C T_1 relaxation time, the 90° rf pulse turns parts or all magnetization for the receiver to be detected. For the saturation recovery, an array of many rf pulses is applied during the saturation block to spoil all magnetization, which then relaxes during the next-following delay t. Therefore, the ^{13}C integral starts negative with short delays for the inversion-recovery and at zero for the saturation recovery. The T_1 can then be calculated from peak integrals or intensities recorded with various delays, t, using a single or double exponential fit (see Eq. 1).

A major drawback of recording all data points to estimate the T_1 is the unreasonable long experiment durations of many days or weeks to reach a sufficiently high signal-to-noise level. As others already reported (Torchia 1978), a CP block prior to the inversion-recovery block enhances the signal-to-noise often twofold (see Fig. 1). The ^1H magnetization is flipped-back after the CP magnetization transfer to allow for a ^{13}C relaxation behavior similar to the methods without CP. However, the delay t should be 4 to 5 times of T_1 to reach the plateau (see Fig. 1c, d) ensuring an accurate estimation of T_1. In case of overlapping peaks and a double exponential T_1 behavior, at least 16 different points needs to be recorded, which is not practical to screen when having a large number of samples.

Results and discussion

Recent ^{13}C NMR studies based on advanced multi-dimensional magic angle spinning (MAS) experiments on uniformly ^{13}C labeled plant cell wall and density functional theory calculations have shed light on the complexity of each broad ^{13}C peak observed in a ^{13}C MAS spectrum (Wang et al. 2014; Yang et al. 2017; Kang et al. 2019). It was reported that one of the C4 peaks arises from the cellulose chains on the surface of a microfibril, sC4, and the other one from the interior, iC4 (Newman and Hemmingson 1994; Wickholm et al. 1998; Wang et al. 2014; Yang et al. 2017; Kang et al. 2019). The remaining surface or interior carbons in an anhydrous glucose unit, must overlap with each other. Hence, it is less surprising that the degree of crystallinity, f_c, corresponding here to the fraction of T_{1c}, obtained from the global fit of the T_1 experiments of MCC and CNC-SO_3H is varying within a peak region (see Fig. 2 top for saturation recovery, red, and inversion-recovery CP, black).

^{13}C T_1 longitudinal relaxation times reflect molecular dynamics on the nanosecond time scale. As expected, and along with others (Dick-Perez et al. 2011), two distinct different T_1s for each peak region were observed. The T_1 of ^{13}C atoms up to 17 s are denoted T_{1a} and are attributed to much faster motions compared to ^{13}C atoms with a T_{1c} with relaxation times up to 130 s (see Table 1). Throughout the text, we will refer to T_{1a} as the 'amorphous' and T_{1c} as the 'crystalline' T_1 although it is important to keep in mind that these relaxation times reflect the difference in mobility, often described as mobile and rigid, as does a CP spectrum and its enhancement (Nowacka et al. 2013).

Notably, the estimated T_{1a} and T_{1c} values of the different carbons for MCC and CNC-SO_3H should be seen as an average of an ensemble of different morphologies. Others have reported that the T_1 might be used as a measure for those (Teeäär and Lippmaa 1984; Newman and Hemmingson 1994; Larsson et al. 1997; Wickholm et al. 1998). In particular for iC4 and sC4, the T_1s are merely an indicator due to the low signal-to-noise. A reliable distribution of T_1s might be obtained with an excellent signal-to-noise and at least 32 variable delay times, which would take several weeks to acquire without ^{13}C enrichment of the cellulose. The degree of crystallinity, f_c, obtained from saturation-recovery T_1 experiments agrees well the

	MCC			
	C1	iC4	sC4	C235
T_{1a} (s)	16.4 ± 0.1	3.47 ± 0.05	1.64 ± 0.02	10.25 ± 0.05
T_{1c} (s)	128.9 ± 1.3	95.6 ± 0.6	54.3 ± 0.2	91.6 ± 0.5
e_{CP}	$1.541 \pm 1 \cdot 10^{-3}$			$1.597 \pm 1 \cdot 10^{-3}$
	CNC-SO$_3$H			
	C1	iC4	sC4	C235
T_{1a} (s)	9.96 ± 0.05	1.94 ± 0.03	7.30 ± 0.05	9.97 ± 0.03
T_{1c} (s)	111.0 ± 0.3	107.9 ± 0.2	67.1 ± 0.3	100.2 ± 0.3
e_{CP}	$2.032 \pm 2 \cdot 10^{-3}$			$2.185 \pm 3 \cdot 10^{-3}$

ones obtained from the inversion-recovery CP T_1 experiments (see Fig. 2 top red and black). Unfortunately, a trustworthy f_c-value of C4 for the inversion-recovery CP T_1 experiment could not be obtained due to the weak signal. However, f_c varied to largest extent for the peak region encompassing the C2, C3 and C5 carbons but no significant difference was found between MCC and CNC-SO$_3$H. In comparison to MCC, CNC-SO$_3$H showed a remarkably larger f_c for C1 while f_c for sC4 was found to be larger for MCC. Hence, C1 appeared more rigid in CNC-SO$_3$H and sC4 in MCC.

The CP enhancement in comparison with DP, e_{CP}, for 1.5 ms contact time obtained from the inversion-recovery T_1 experiments, was in the range 2.0–2.2 for CNC-SO$_3$H and 1.5–1.6 for MCC. These values agreed well with e_{CP} values estimated from the comparison of 1D CP and DP experiments (see Table 2). The e_{CP} values were similar for C1 and C235 for all samples but a significant difference up to 30% was found for iC4 and sC4 for MCC and CNC-SO$_3$H (see Figure S2 for a visual examination). CNC-SO$_3$H and soaked MCC, MCC$_{wet}$, showed the largest e_{CP}. The e_{CP} varied significantly for the different

samples (see Table 2) but less for the different carbon peak regions (see Fig. 2).

The C6 region is excluded from evaluation because the CH$_2$ group has a larger degree of freedom and is not part of the cellulose ring yielding a T_{1a} of only a couple of seconds and a T_{1c} between 30 and 70 s. Nevertheless, there is a difference in T_{1a} and T_{1c}, facilitating another relaxation filter. The difference in e_{CP} between samples might be caused by a change in mobility on the millisecond time scale or a change of the order parameter S, the preferred orientation of the ^{1}H–^{13}C bond (Nowacka et al. 2013). Dick-Perez et al. (2011) reported on an order parameter of 0.8 for cellulose in the plant cell wall.

As presented in Table 1, there is a T_1 difference of one order of magnitude between 'amorphous' and 'crystalline' signals of the investigated carbon peaks. Hence, a T_1 filter in combination with an inversion-recovery CP to enhance signal might be used to estimate the degree of crystallinity, f_c. The simulated integrals for the inversion-recovery CP method (see Fig. 1c), with an e_{CP} of 2.5, start at $I(0) = -2.5$ but end at 1 due to the similar ^{13}C relaxation mechanism as for DP during the delay t after the ^{1}H flip-back pulse.

	C1	C235	iC4	sC4
MCC	1.27 ± 0.02	1.26 ± 0.01	1.32 ± 0.02	1.05 ± 0.02
MCC$_{wet}$	2.47 ± 0.12	2.55 ± 0.05	2.79 ± 0.15	2.30 ± 0.16
MCC$_{ex}$	1.17 ± 0.02	1.24 ± 0.01	1.41 ± 0.03	1.26 ± 0.03
Cell$_{Am}$	1.47 ± 0.14	1.86 ± 0.09	–	2.13 ± 0.42
CNC-SO$_3$H	2.36 ± 0.04	2.41 ± 0.02	2.71 ± 0.06	1.95 ± 0.04

For a specific delay, t_{a0}, the ^{13}C integrals arising from the amorphous cellulose chain are at zero net magnetization while the crystalline signals, I_{ta0}, are still negative. Since the ^{13}C T_1 of the rigid 'crystalline' signals are known, we can calculate the remaining negative magnitude of the rigid 'crystalline' signals at t_{a0} using

$$m_{ta0} = 1 - p \cdot e^{-t_{a0}/T_{1c}} \quad (2)$$

where T_{1c} 100 s was used and p is $1 + e_{CP}$ because at t_{a0} the second term in Eq. 1 is zero making it easy to solve for the crystallinity f_c from the remaining first term. To estimate $f_{c.inv}$, a ^{13}C CP spectrum with the same number of accumulated scans is required, which comprises the total amount of signal I_{tot}, with an experimental duration of 5 min. Hence, $f_{c.inv}$ is calculated as follows

$$f_{c.inv} = e_{CP}/m_{ta0} \cdot I_{ta0}/I_{tot}. \quad (3)$$

The first part of the equation, e_{CP}/m_{ta0}, is needed to rescale I_{tot} to the DP scale since the signals relax to 1 in the inversion-recovery CP experiment.

A downside of the inversion-recovery CP method is that e_{CP} needs to be estimated in order to find $t_{a0} = -\ln(1/p) \cdot T_{1a}$. The e_{CP} varies strongly with the mobility of the ^{13}C–^{1}H bond and its order parameter S (Nowacka et al. 2013). The e_{CP} can be estimated by using the difference in intensity of a ^{13}C CP experiment, the same which is used for I_{tot}, and a ^{13}C DP experiment with a repetition delay of at least 400 s, which is time-consuming. For accuracy, the ^{13}C spectra require a reasonable signal-to-noise, which was obtained with 128 signal accumulations in this setup. The latter experiment took 14 h while the first one took 5 min. The experiment with the optimal t_{a0} took about 40 min. If the cellulose samples are similar, the e_{CP} might only be estimated for one sample.

The degree of crystallinity, $f_{c.sat}$, might also be derived from saturation-recovery experiments. For this method, a saturation-recovery experiment was needed to be recorded with a delay t of 109 s, at which the carbons from the amorphous cellulose chains were allowed to relax completely (see Fig. 1d). However, the delay t could be further optimized to save time. The degree of crystallinity is calculated as follows

$$f_{c.sat} = \{1 - (I_{109s}/I_{400s})\} \cdot e^{109/T_{1c}} \quad (4)$$

where I_{109s} is the integral with a delay t of 109 s and I_{400s} the corresponding value at 400 s. Although the approximation of e_{CP} is not needed, background signals and low signal-to-noise complicate the accuracy of this method. The total experimental duration was 19 h.

In addition the ^{13}C $T_{1\rho}$ was examined as a parameter, which would provide shorter experiment durations but a strong dependence on the spinlock field and very short $T_{1\rho}$ relaxation times complicate a meaningful implementation.

The uncertainty of f_c due to missetting of T_{1a}, T_{1c} and e_{CP} for both methods was simulated for given T_{1a}, T_{1c} and e_{CP} (see Fig. 3). For the inversion-recovery CP method, T_{1a} seems to be the crucial parameter while T_{1c} and e_{CP} have minor effect on f_c. However, the accurate setting of the t_{a0} delay, which depends on T_{1a} and e_{CP} is easily judged visually. Hence the inversion-recovery CP method seems promising. If the delay would be wrong, positive ^{13}C signals would be observed (see Fig. 4a). In contrast, the saturation-recovery method is vulnerable to very small differences in T_{1c} and to obtain an accurate value T_{1c} is very time-consuming.

The ^{13}C inversion-recovery CP signals of CNC-SO$_3$H (see Fig. 4a, red) are negative and the CP spectrum with a repetition delay of 2 s displays
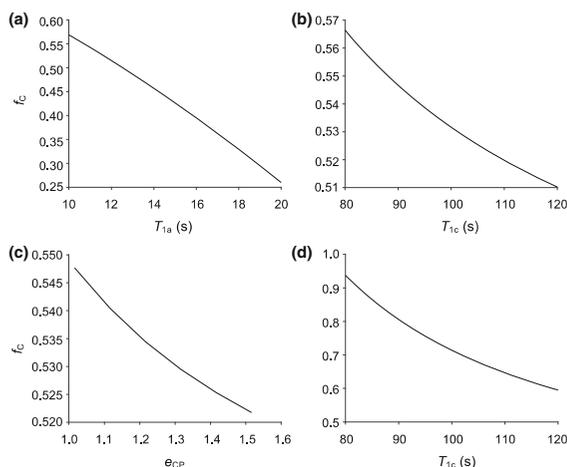

Fig. 3 Simulations of f_c as a function of amorphous T_{1a}, crystalline T_{1c} and CP enhancement e_{CP} for inversion-recovery CP method (**a–c**) for a given e_{CP} of 1.27, T_{1a} 15 s and T_{1c} of 100 s and as a function of T_{1c} for the saturation-recovery method (**d**)
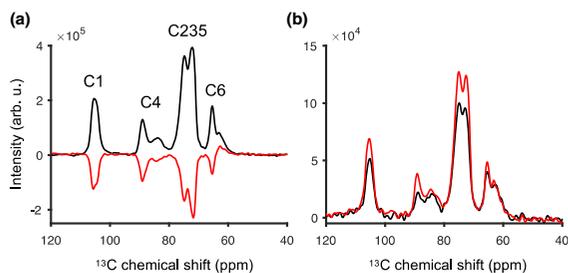
Fig. 4 ^{13}C spectra of CNC-SO$_3$H. CP spectrum with a repetition delay of 2 s (**a**, black) and inversion-recovery CP spectrum with a t_{a0} of 18.3 s (**a**, red). Saturation-recovery spectrum with a variable delay of 109 s (**b**, black) and a DP spectrum with a repetition delay of 400 s (**b**, red)

positive signals (see Fig. 4a, black). The saturation-recovery spectra reveal solely positive signals with little difference in intensities for the two different delays, 109 and 400 s (see Fig. 4b, black and red). Similar spectra were obtained for the remaining samples. The saturation-recovery experiments are in general noisier due to the absent CP enhancement.

The two methods described above were applied to the five different cellulose samples and compared the results with the integration and deconvolution NMR based methods as well as WAXS. The WAXS patterns of MCC and CNC-SO$_3$H appeared more or less identical (Fig. 5) while the Cell$_{Am}$ pattern lack any features. The same degree of crystallinity, $f_{c.x} = 0.54$, was obtained for MCC$_{ex}$ and MCC$_{wet}$. MCC had a slightly lower value of 0.52 while CNC-SO$_3$H had the lowest with 0.48 (see Table 3). Ahvenainen et al. (2016) have shown that the estimated degree of crystallinity using WAXS is dependent on the crystallite size distribution. Hence, the lower $f_{c.x}$ for CNC-SO$_3$H might be motivated by the expected smaller crystallites in CNC-SO$_3$H. No WAXS-crystallinity analysis was performed on the alcohol coagulated amorphous cellulose since the fitting model does no longer apply. However, visual inspection of the Cell$_{Am}$ WAXS pattern revealed a low degree of crystallinity. It should be known that cellulose crystallinity measurements from X-ray patterns can never be directly compared with NMR methods due to the crystalline size interaction and choice of analysis method affecting the final crystallinity result. However it can still be useful to do so since Avicell PH-101 is a commercial product that can be used by anyone to repeat our experiments.
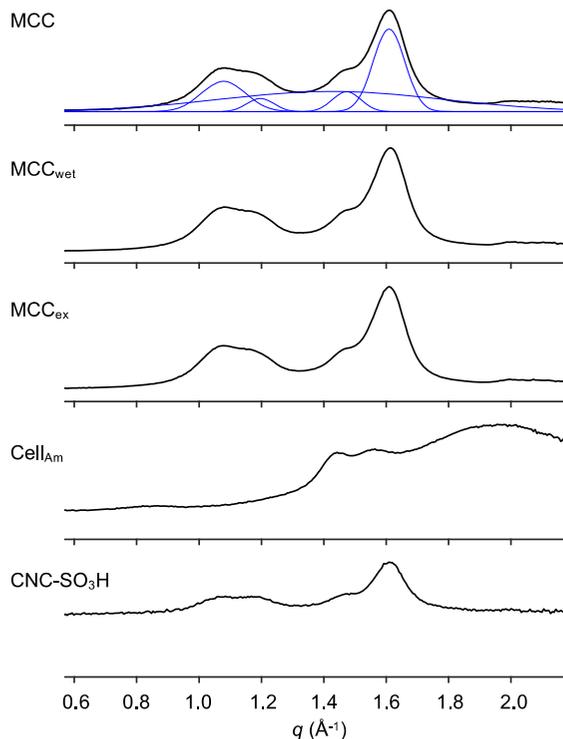

Fig. 5 Wide-angle X-ray scattering pattern for MCC, MCC$_{wet}$, MCC$_{ex}$, Cell$_{Am}$ and CNC-SO$_3$H

The estimated degrees of crystallinity, $f_{c.inv}$, $f_{c.sat}$, $f_{c.int}$ and $f_{c.dec}$, are summarized in Table 3. Except from the amorphous cellulose sample, the lowest degree of crystallinity $f_{c.inv}$ was observed for the MCC and MCC$_{ex}$, whose labile hydroxyl hydrogens were exchanged from ^1H to ^2H. CNC-SO$_3$H appeared slightly more crystalline compared to MCC and the addition of water seems to impact the crystallinity positively. There are only small variations between the different carbon atom regions.

The degree of crystallinity $f_{c.sat}$ obtained from saturation-recovery experiments differs significantly from $f_{c.int}$ except for the CNC-SO$_3$H sample. As mentioned earlier, these spectra are noisier resulting in a larger error, while the background signal of the probe and rotor contributes to the integration. A slight difference in T_{1c} could also explain the different results.

$f_{c.int}$ based on the integration method is calculated from the ratio of the two C4 signals and differs about 10% compared to $f_{c.inv}$ expect for MCC$_{wet}$. This method works only if e_{CP} is the same for both signals. The same is true for the deconvolution method, which

Table 3 Estimated degree of crystallinity, $f_{c.inv}$, $f_{c.sat}$, $f_{c.int}$, $f_{c.dec}$ and $f_{c.x}$ for five different cellulose samples

	C1	C235	C4 (iC4 and sC4)	WAXS
MCC				
$f_{c.inv}$	0.53 ± 0.01	0.49 ± 0.01	0.52 ± 0.01	–
$f_{c.sat}$	0.73 ± 0.07	0.64 ± 0.03	0.83 ± 0.09	–
$f_{c.int}$	–	–	0.57 ± 0.01	–
$f_{c.dec}$	–	–	–	–
$f_{c.x}$	–	–	–	0.52 ± 0.02
MCC$_{wet}$				
$f_{c.inv}$	0.60 ± 0.01	0.57 ± 0.01	0.60 ± 0.01	–
$f_{c.sat}$	0.70 ± 0.11	0.66 ± 0.04	0.79 ± 0.13	–
$f_{c.int}$	–	–	0.60 ± 0.01	–
$f_{c.dec}$	–	–	0.56 ± 0.07	–
$f_{c.x}$	–	–	–	0.54 ± 0.02
MCC$_{ex}$				
$f_{c.inv}$	0.49 ± 0.04	0.48 ± 0.02	0.50 ± 0.06	–
$f_{c.sat}$	0.89 ± 0.10	0.69 ± 0.04	0.73 ± 0.13	–
$f_{c.int}$	–	–	0.57 ± 0.01	–
$f_{c.dec}$	–	–	–	–
$f_{c.x}$	–	–	–	0.54 ± 0.02
Cell$_{Am}$				
$f_{c.inv}$	–0.14 ± 0.02	–0.05 ± 0.01	–	–
$f_{c.sat}$	0.10 ± 0.35	0.28 ± 0.14	–	–
$f_{c.int}$	–	–	–	–
$f_{c.dec}$	–	–	–	–
$f_{c.x}$	–	–	–	–
CNC–SO$_3$H				
$f_{c.inv}$	0.63 ± 0.01	0.59 ± 0.01	0.64 ± 0.02	–
$f_{c.sat}$	0.68 ± 0.06	0.60 ± 0.03	0.86 ± 0.09	–
$f_{c.int}$	–	–	0.58 ± 0.01	–
$f_{c.dec}$	–	–	–	–
$f_{c.x}$	–	–	–	0.48 ± 0.03

gave a $f_{c.dec}$ of 0.56 for MCC$_{wet}$. The deconvolution method works solely for wet samples as it requires sharp lineshapes.

The $f_{c.x}$ from the WAXS results are similar as the $f_{c.inv}$ except for CNC-SO$_3$H. As mentioned earlier, one reason might be a smaller crystal size compared to the MCC samples. It should be emphasized again that WAXS uses the scattering of X-rays to estimate the degree of crystallinity while CP-based NMR methods independently on the integration, deconvolution or the presented inversion-recovery method observes a difference in mobility. Although WAXS takes only 30 min to record, the WAXS pattern must be deconvoluted. Our proposed method, if similar cellulose samples, could be applied routinely using a sample changer to measure a lot of samples.

Conclusion

By this work, a solid-state NMR method is proposed to obtain degree of crystallinity for cellulose, both native and regenerated. The method is based on ^{13}C NMR as a mobility indicator due to the large difference in local mobility between rigid (crystalline) and mobile (amorphous) cellulose material. An inversion-

recovery CP method described here allows, by applying a T_1 filter, to access the degree of crystallinity after estimating the CP signal enhancement. The routine is user-friendly since only a spectral integral has to be calculated, which is fed into a simple equation and the degree of crystallinity is obtained for all carbons apart from C6. Measurement time is drastically reduced compared to contemporary solid-state NMR experiments if the CP enhancement is known and enables a high-throughput of samples if the magnet is equipped with a sample changer. The results also recommend, in agreement with the recent literature, that the integral method of the C4 peak might be used if a similar CP enhancement of all peaks is assured.

References

Ahvenainen P et al (2016) Comparison of sample crystallinity determination methods by X-ray diffraction for challenging cellulose I materials. Cellulose 23:1073–1086

Dick-Perez M et al (2011) Structure and interactions of plant cell-wall polysaccharides by two- and three-dimensional magic-angle-spinning solid-state NMR. Biochemistry 50(6):989–1000

Dufrense A (2017) Nanocellulose from nature to high performance tailored materials. De Gruyter, Berlin

Evans R et al (1995) Changes in cellulose crystallinity during kraft pulping. Comparison of infrared, X-ray diffraction and solid state NMR results. Holzforschung 49:498–504

Ferreira TM et al (2015) Model-free estimation of the effective correlation time for C–H bond reorientation in amphiphilic bilayers: ^{1}H-^{13}C solid-state NMR and MD simulations. J Chem Phys 142

Fung BM et al (2000) An improved broadband decoupling sequence for liquid crystals and solids. J Magn Reson 142:97–101

Hasani M et al (2008) Cationic surface functionalization of cellulose nanocrystals. Soft Matter 4(11):2238–2244

Idström A et al (2016) ^{13}C NMR assignments of regenerated cellulose from solid-state 2D NMR spectroscopy. Carbohydr Polym 151:480–487

Kang X et al (2019) Lignin-polysaccharide interactions in plant secondary cell walls revealed by solid-state NMR. Nat Commun 10:347

Kim J-W et al (2013) Structure and thermomechanical properties of stretched cellulose films. J Appl Polym Sci 128:181–187

Klemm D et al (2005) Cellulose: fascinating biopolymer and sustainable raw material. Angew Chem Int Ed 44:3358–3393

Klemm D et al (2011) Nanocelluloses: a new family of nature-based materials. Angew Chem Int Ed 50:5438–5466

Larsson TP et al (1997) A CP/MAS ^{13}C NMR investigation of molecular ordering in celluloses. Carbohydr Res 302:19–25

Larsson TP et al (1999) CP/MAS ^{13}C-NMR spectroscopy applied to structure and interaction studies on cellulose I. Solid State Nucl Magn Reson 15:31–40

Liitiä T et al (2000) Solid state NMR studies on cellulose crystallinity in fines and bulk fibres separated from refined kraft pulp. Holzforschung 54:618–624

Liitiä T et al (2003) Cellulose crystallinity and ordering of hemicelluloses in pine and birch pulps as revealed by solid-state NMR spectroscopic methods. Cellulose 10:307–316

Newman RH (1999) Estimation of the lateral dimensions of cellulose crystallites using ^{13}C NMR signal strenghts. Solid State Nucl Magn Reson 15:21–29

Newman RH, Hemmingson JA (1994) Carbon-13 NMR distinction between categories of molecular order and disorder in cellulose. Cellulose 2:95–110

Nowacka A et al (2013) Signal intensities in ^{1}H–^{13}C CP and INEPT MAS NMR of liquid crystals. J Magn Reson 230:165–175

Östlund Å et al (2013) Modification of crystallinity and pore size distribution in coagulated cellulose films. Cellulose 20:1657–1667

Park S et al (2009) Measuring the crystallinity index of cellulose by solid state ^{13}C nuclear magnetic resonance. Cellulose 16:641–647

Park S et al (2010) Cellulose crystallinity index: measurement techniques and their impact on interpreting cellulase performance. Biotechnol Biofuels 3:10

Röder T et al (2006) Crystallinity determination of native cellulose—comparision of analytical methods. Lenzinger Ber 86:85–89

Schantz S (1997) Structure and mobility in poly(ethylene oxide)/poly(methylmethacrylate) blends investigated by ^{13}C solid-state NMR. Macromolecules 30:1419–1425

Schenzel K et al (2005) New method for determining the degree of cellulose I crystallinity by means of FT Raman spectroscopy. Cellulose 12:223–231

Sixta H et al (2015) Ioncell-F: a high-strength regenerated cellulose fibre. Nord Pulp Pap Res J 30(1):43–57

Teeäär R, Lippmaa E (1984) Solid state ^{13}C-NMR of cellulose. A relaxation study. Polym Bull 12:315–318

Torchia DA (1978) The measurement of proton-enhanced carbon-13 T_1 values by a method which supresses artifacts. J Magn Reson 30:613–616

Wang T et al (2014) Structure and dynamics of brachypodium primary cell wall polysaccharides from two-dimensional ^{13}C solid-state nuclear magnetic resonance spectroscopy. Biochemistry 53:2840–2854

Wickholm K et al (1998) Assignment of non-crystalline forms in cellulose I by CP/MAS ^{13}C NMR spectroscopy. Carbohydr Res 312:123–129

Yang H et al (2017) Structural factors affecting ^{13}C NMR chemical shifts of cellulose: a computational study. Cellulose 25:23–36